microbial biotechnology

Open Access

Oligomerization engineering of the fluorinase enzyme leads to an active trimer that supports synthesis of fluorometabolites *in vitro*

Tiia Kittilä,[1] Patricia Calero,[1] Folmer Fredslund,[1] Phillip T. Lowe,[2] David Tezé,[1] Manuel Nieto-Domínguez,[1] David O'Hagan,[2] Pablo I. Nikel[1,*] and Ditte H. Welner[1,]**

[1]*The Novo Nordisk Foundation Center for Biosustainability, Technical University of Denmark, Kongens Lyngby, 2800, Denmark.*

[2]*School of Chemistry, University of St. Andrews, St. Andrews, KY16 9ST, UK.*

Summary

The fluorinase enzyme represents the only biological mechanism capable of forming stable C–F bonds characterized in nature thus far, offering a biotechnological route to the biosynthesis of value-added organofluorines. The fluorinase is known to operate in a hexameric form, but the consequence(s) of the oligomerization status on the enzyme activity and its catalytic properties remain largely unknown. In this work, this aspect was explored by rationally engineering trimeric fluorinase variants that retained the same catalytic rate as the wild-type enzyme. These results ruled out hexamerization as a requisite for the fluorination activity. The Michaelis constant (K_M) for *S*-adenosyl-L-methionine, one of the substrates of the fluorinase, increased by two orders of magnitude upon hexamer disruption. Such a shift in *S*-adenosyl-L-methionine affinity points to a long-range effect of hexamerization on substrate binding – likely decreasing substrate dissociation and release from the active site. A practical application of trimeric fluorinase is illustrated by establishing *in vitro* fluorometabolite synthesis in a bacterial cell-free system.

Received 4 December, 2021; revised 12 January, 2022; accepted 14 January, 2022.

For correspondence. *E-mail pabnik@biosustain.dtu.dk; **E-mail diwel@biosustain.dtu.dk; Tel. (+45 93) 51 19 18; Fax (+45 45) 25 80 00.

Microbial Biotechnology (2022) **15**(5), 1622–1632
doi:10.1111/1751-7915.14009

Funding Information

This work was funded by The Novo Nordisk Foundation grant to the Center for Biosustainability (NNF10CC1016517). P.I.N. was funded by grants from The Novo Nordisk Foundation (NNF20CC0035580, and *LiFe*, NNF18OC0034818), the European Union's Horizon 2020 Research and Innovation Programme under grant agreement No. 814418 (*SinFonia*) and the Danish Council for Independent Research (*SWEET*, DFF-Research Project 8021-00039B). T.K. and M.N.D. were funded by fellowships from the European Union's Horizon 2020 research and innovation program under a Marie Skłodowska Curie project under grant agreement No. 713683 (*COFUNDfellowsDTU*).

Introduction

Organohalides (i.e., organic molecules containing halogens) are essential chemical building blocks for the synthesis of pharmaceuticals, materials and agrochemicals, an occurrence highlighted by the fact that over 25% of blockbuster drugs display fluorine (F) atoms in their structures (Martinelli and Nikel, 2019; Mei *et al.*, 2019; Johnson *et al.*, 2020). F is the most electronegative element in the Periodic Table, and the C–F bond is the strongest covalent bond involving C (O'Hagan, 2008; Cros *et al.*, 2022). Substituting hydrogen (H) atoms with F has a relatively low steric impact – however, F exchange greatly influences the acidity/basicity, hydrophobicity, conformation and reactivity of organofluorine compounds relative to the non-fluorinated hydrocarbon structures (Purser *et al.*, 2008; Pimviriyakul *et al.*, 2020; Wu *et al.*, 2020). These modifications translate into improved pharmacokinetic parameters such as metabolic stability, increased binding to target molecules and/or improved membrane permeability when compared to the analogous non-fluorinated compound (Meanwell, 2018; Johnson *et al.*, 2020). Organic chemistry methods exist for the synthesis of organofluorines and, more often than not, these require hazardous and noxious reagents. It follows that there are attractive prospects for the development of a biotechnology in this area (Cheng and Ma, 2021), but this goal is presently challenged by very limited access to appropriate enzymatic routes towards organofluorine biosynthesis. As such, developing a biotechnology for the site-selective introduction of F into structurally diverse molecules would circumvent the harsh chemistry associated with chemical fluorination, and remains one of the great goals in metabolic engineering (Wu *et al.*, 2020). So far, the fluorinase [FlA, 5'-fluoro-5'-deoxyadenosine (5'-FDA) synthase], isolated from *Streptomyces* and related Gram-positive bacterial species, is the only known enzyme capable of forming stable C–F bonds (O'Hagan *et al.*, 2002; Dong *et al.*, 2004). FlA catalyses the formation of 5'-FDA through a

© 2022 The Authors. *Microbial Biotechnology* published by Society for Applied Microbiology and John Wiley & Sons Ltd.
This is an open access article under the terms of the Creative Commons Attribution-NonCommercial-NoDerivs License, which permits use and distribution in any medium, provided the original work is properly cited, the use is non-commercial and no modifications or adaptations are made.

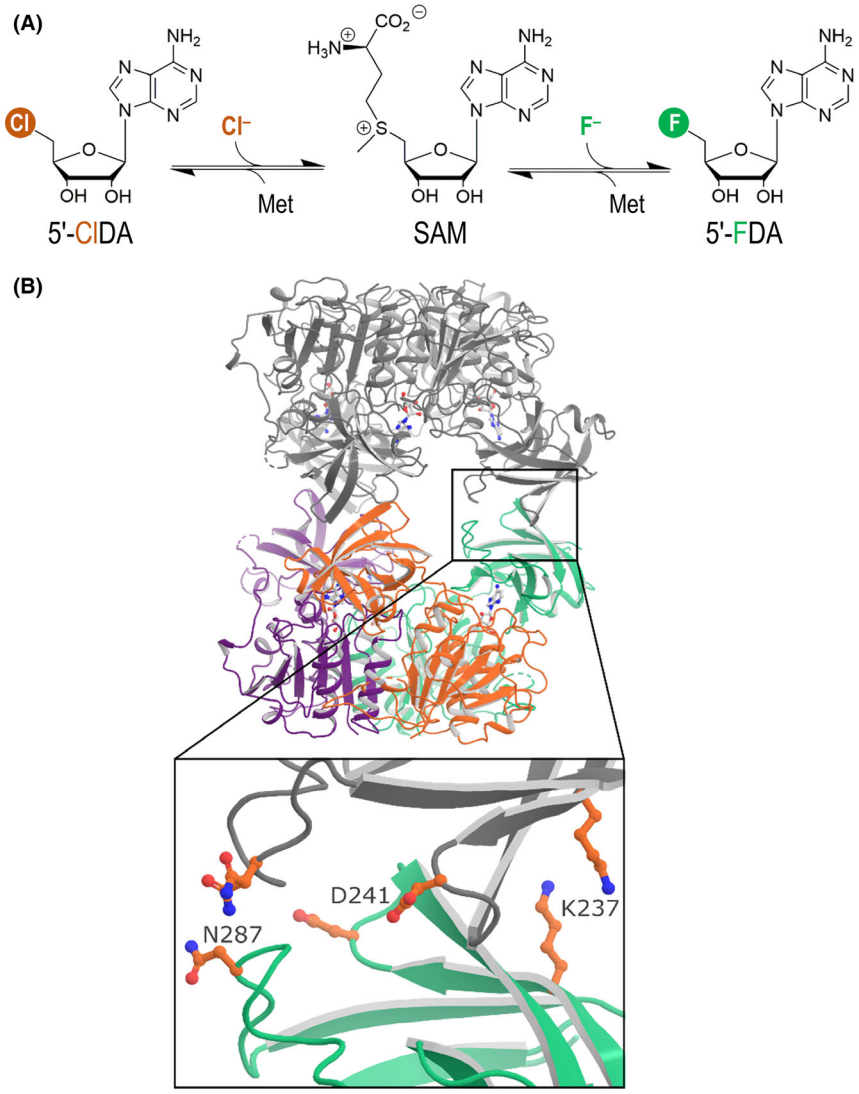

Fig. 1. A. Reactions catalysed by the fluorinase enzyme. Abbreviations are as follows: Cl^-, chloride ion; F^-, fluoride ion; SAM, *S*-adenosyl-L-methionine; Met, L-methionine; 5'-ClDA, 5'-chloro-5'-deoxyadenosine; and 5'-FDA, 5'-fluoro-5'-deoxyadenosine.
B. A 3D model of the FIA fluorinase enzyme from *Streptomyces* sp. strain MA37. The amino acid residues sitting at the trimer-trimer interface, critical for the formation of the hexameric form, are highlighted in the inset.

nucleophilic attack of the fluoride ion (F^-) on the electrophilic C5' carbon of *S*-adenosyl-L-methionine (SAM, the universal methyl donor), thereby releasing L-methionine (Met) through an S_N2 reaction mechanism (Fig. 1A). FIA also catalyses the formation of SAM from 5'-chloro-5'-deoxyadenosine (5'-ClDA) and Met as the substrates (O'Hagan and Deng, 2015; Sun *et al.*, 2018) – that is, in the reverse reaction direction.

FIA has been successfully implemented *in vitro* (Sun *et al.*, 2016; Carvalho and Oliveira, 2017) for a number of practical applications, for example, in the preparation of ^{18}F-labelled peptides for positron emission tomography (Liang *et al.*, 2013). Additionally, this halogenase has been used for *in vivo* fluorometabolite biosynthesis in engineered bacterial cell factories (Eustáquio *et al.*, 2010; Calero *et al.*, 2020; Markakis *et al.*, 2020). Yet, the applications of FIA have been hampered by its narrow substrate scope and low catalytic efficiency (with a turnover number k_{cat} = 0.08–0.26 min^{-1}; Deng *et al.*, 2004; Cobb *et al.*, 2006; Nieto-Domínguez and Nikel, 2020). Crystal structures of FIA indicate that the enzyme forms a hexamer consisting of a dimer of trimers (Fig. 1B; Dong *et al.*, 2004; Deng *et al.*, 2006). The FIA fluorinase has also been described to exist as a hexamer in its native form in solution (Deng *et al.*, 2014). According to this interpretation, three active sites are situated at the interfaces between adjacent monomers in the trimer, while the trimer-trimer interface has no

© 2022 The Authors. *Microbial Biotechnology* published by Society for Applied Microbiology and John Wiley & Sons Ltd.,

obvious catalytic function (Fig. 1B). This observation on the structural features of FlA, together with the fact that a homologous chlorinase enzyme (SalL) forms a functional trimer while displaying a k_{cat}/K_M specificity constant 100-fold higher than that of the fluorinase (Eustáquio *et al*., 2008), led us to investigate the role of FlA hexamerization on catalysis. The few other fluorinase enzymes described in the literature have not been characterized in detail thus far (e.g., by crystallographic analysis), and the oligomerization status of these halogenases remain to be explored (Cheng and Ma, 2021). On this background, in this article we report our efforts towards rational deconstruction of the hexameric form of the FlA fluorinase. By introducing a number of rationally engineered mutations in the enzyme structure, we show how the formation of the hexamer is not a requisite for the catalytic activity. Moreover, we demonstrate that trimeric variants of FlA can be harnessed for the biosynthesis of fluoronucleotides in an *in vitro*, cell-free bacterial system as a practical application example.

Results

Rational design, construction and testing of FlA mutants

With a view to disrupt hexamerization of the fluorinase while preserving intact trimers, we designed eight FlA variants guided by sequence alignments and the crystal structures of the archetypal FlA from *Streptomyces* sp. strain MA37 [PDB ID 5LMZ] (Deng *et al*., 2014) and the SalL chlorinase from *Salinispora tropica* [PDB ID 2Q6K] (Eustáquio *et al*., 2008). All of the engineered mutations are located at the trimer-trimer interface of the fluorinase, and they were designed to substitute FlA residues with the corresponding SalL amino acids at key positions while considering electrostatic forces as part of the design principles (Table 1). We constructed these mutant versions of FlA by mutagenesis PCR (see Experimental Procedures), introducing either point mutations (individually or in combination) or by insertional mutagenesis. Four of these engineered variants (which were termed FlA-K237E, FlA-D241A, FlA-K237E/N287P and FlA-242_243InsLS) could be successfully produced in *Escherichia coli* BL21 and purified with high protein mass yields. We started the characterization of the enzyme variants by testing the ability of each FlA mutant to mediate the forward (i.e., fluorination) and reverse (i.e., SAM formation) reaction by exposing the purified enzymes to the corresponding substrates. In these experiments, either SAM or 5'-ClDA were used as the substrate to assess the forward or reverse reaction catalysed by FlA respectively. The reaction mixture also contained KF (as the source of F^- ions for the forward reaction), L-Met (for the reverse reaction starting with 5'-ClDA) and NaCl. After incubating the reaction mixtures for 4 h, the products (i.e., 5'-FDA or SAM) were detected and quantified by HPLC. Under these assay conditions, we observed that each of the variants could catalyse the formation of 5'-FDA from SAM and F^-, although both the FlA-K237E/N287P and FlA-242_243InsLS mutants displayed considerably lower activity than wild-type FlA (Fig. 2). In the former case (i.e., combined point mutations), the residual activity was almost negligible, whereas FlA-242_243InsLS had a approximately 80% reduction in the catalytic output as compared to the wild-type fluorinase. SAM formation from 5'-FDA, on the other hand, was impaired for the FlA-K237E, FlA-K237E/

Table 1. Mutant FlA variants designed in this study.[a]

FlA mutant	Design rationale
K237E	Disruption of the trimer:trimer hydrogen bond to E247
D241A	Disruption of the trimer:trimer hydrogen bond to Y286
K237E/D241A	Disruption of both hydrogen bonds above
242_243InsLS	Extending the trimer:trimer interface loop with residues from chlorinase
K237E/N287P	N287P disrupts backbone interaction with the other trimer; 287 is close to itself
K237E/I263P	I263P mimics chlorinase structure
K237E/L244T	L244T mimics chlorinase structure and disrupts hydrophobic packing; 244 is close to itself
K237E/I263P/ L244T	Combination of all the rational mutations above

a. All mutant FlA were constructed by mutagenesis PCR using the *flA* gene from *Streptomyces* sp. strain MA37 as the template.

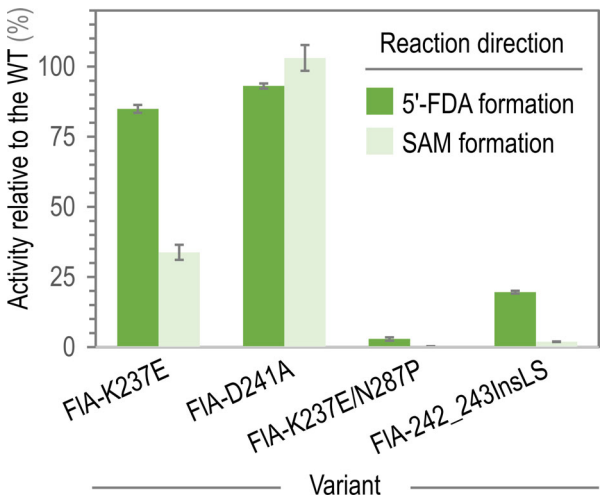

Fig. 2. Activity of rationally engineered FlA variants relative to the wild-type (WT) FlA fluorinase. Each variant was tested both in the direction of 5'-FDA (5'-fluoro-5'-deoxyadenosine) formation (i.e., direct C–F bond formation) and in the reverse direction [i.e., *S*-adenosyl-L-methionine (SAM) formation from 5'-chloro-5'-deoxyadenosine]. Results represent average values of the relative enzymatic activity and the error bars indicate standard deviations from at least three independent biological replicates.

© 2022 The Authors. *Microbial Biotechnology* published by Society for Applied Microbiology and John Wiley & Sons Ltd.,

N287P and FIA-242_243InsLS variants. The FIA-D241A mutant, in turn, retained the activity of the wild-type enzyme in both reaction directions (Fig. 2), indicating a high degree of reversibility in its catalytic activity. Based on these results, the FIA-K237E variant emerged as the most interesting one to explore trimer-based fluorination. The next question was to analyse the actual oligomeric state of these fluorinase variants.

Biophysical exploration of the oligomerization state of FIA and its engineered variants

The oligomerization state of proteins is critical to their function, forming the basis for substrate recognition and underpinning the biophysical phenomena of allostery and cooperativity (Goodsell and Olson, 2000; Liu *et al.*, 2020). Understanding the mechanism and pathways by which proteins assemble into higher order structures is critical both from a fundamental and applied point of view. Several biochemical and biophysical methods are available to examine the oligomerization behaviour of proteins. To study the oligomerization state of FIA and the set of mutants constructed herein, we resorted to both size-exclusion chromatography (SEC) and small-angle X-ray scattering (SAXS) methodologies (Gell *et al.*, 2012; Blanchet and Svergun, 2013).

The FIA variants were firstly subjected to SEC analysis (Fig. 3A). The purified FIA eluted as two distinct peaks of different intensity. We interpreted the appearance of the first and predominant peak to represent a hexameric population (within the 12–16 ml range), while the second peak – which has not been described previously – appears to be a trimeric subpopulation. In this case, approximately 75% of the purified protein sample was found to correspond to the hexameric population, as determined by the area under the curve (Fig. 3A). To substantiate this observation, we subjected the wild-type FIA to SEC coupled to SAXS (Fig. 4A). Guinier analysis (Zheng and Best, 2018) of the scattering curve resulting from the major peak gave a radius of gyration (R_g, in Å) and maximum distance (D_{max}, in Å) fully compatible with a hexamer (Fig. 3B). A poor fit to the theoretical scattering curve in the mid-*s* (scattering) range [evaluated as the squared Chi value (χ^2) of the fitting curve, Fig. 4A] indicates some deviation in the overall shape of the wild-type FIA enzyme with respect to the reported crystal structure (Dong *et al.*, 2004). The minor peak from wild-type FIA, however, did not contain enough material to obtain a meaningful scattering curve.

In contrast with wild-type FIA, all four engineered variants gave rise to a predominant peak in SEC experiments corresponding to the assumed trimeric population (located around 14 ml, Fig. 3A). We leveraged this feature to obtain a scattering curve from the trimer peak

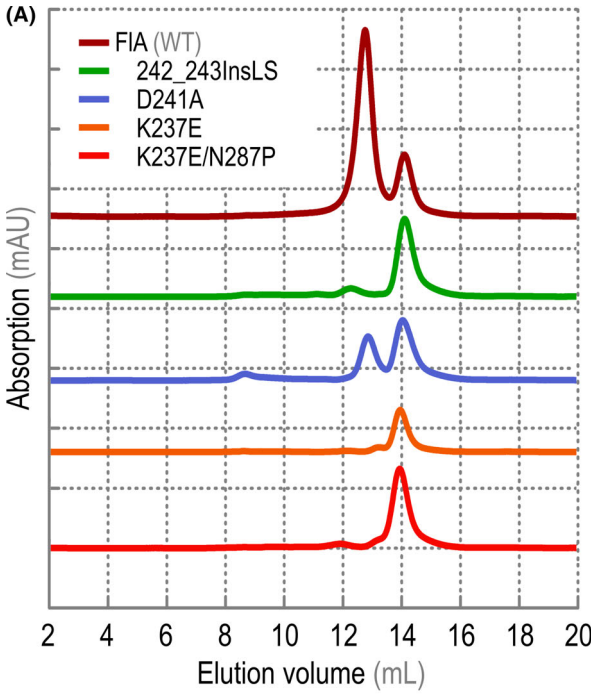

(B)

Fluorinase variant	R_g (Å)	D_{max} (Å)
FIA (WT)	38.5	106.9
FIA-K237E	31.7	89.0
Hexamer	38.0	114.2
Trimer	28.1	85.3

Fig. 3. A. Analysis of wild-type (WT) FIA and rationally engineered mutants by means of size-exclusion chromatography (SEC). Absorption values are indicated as *mAU*, arbitrary intensity units $\times 10^{-3}$.
B. Experimentally determined radius of gyration (R_g) and maximum size (D_{max}) of the WT FIA and the FIA-K237E variant deduced from small-angle X-ray scattering (SAXS) data (see Fig. 4). R_g and D_{max} values for a pure hexamer and trimer are likewise included in the table for comparison.

(Fig. 4B). Guinier analysis of scattering data from the major peak observed for the FIA-K237E variant indeed fitted well with a proposed trimer (Fig. 3B). Again, a poor fit to the theoretical scattering curve in the mid-*s* range indicated some shape deviation in solution from the reported crystal structure. In addition to the predominant trimeric population, all variants displayed low amounts of high molecular weight species or potential aggregates. Furthermore, preparations of FIA-D241A had a significant level (approximately 33%) of hexamer, indicating an only partial disruption of this predominant oligomeric form – a feature that may correlate with the highly reversible activity profile observed for this variant (Fig. 2). Samples of the FIA-K237E, FIA-K237E/N287P and FIA-242_243InsLS variants showed a single peak compatible

© 2022 The Authors. *Microbial Biotechnology* published by Society for Applied Microbiology and John Wiley & Sons Ltd.,

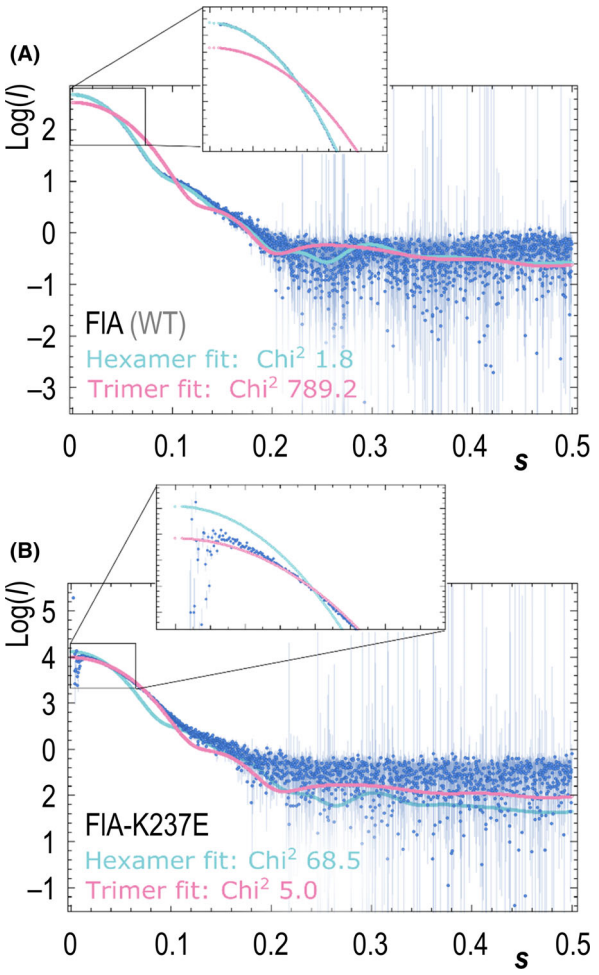

Fig. 4. Small-angle X-ray scattering (SAXS) profiles for (A) the wild-type (WT) fluorinase and (B) the trimeric variant FIA-K237E. The plots represent the logarithm of the scattering intensity (*I*, arbitrary units) as a function of momentum transfer (*s*, in $Å^{-1}$), along with the best adjustment that fits to the experimental data according to the two possible oligomerization states. Squared Chi values (χ^2) for these mathematical adjustments are included for both the hexamer and the trimer model.

with the trimeric form of the fluorinase. Prompted by these results, we selected the FIA-K237E variant, which had both the highest activity in the forward reaction (Fig. 2) and showed a SEC-SAXS profile compatible with a pure trimer (Figs 3 and 4), for further analysis of kinetic parameters.

Kinetic properties of the rationally engineered FIA mutants

As indicated above, the FIA-K237E fluorinase variant was almost exclusively found as a trimer in solution (approximately 97%) yet it retained >80% of the wild-type activity in assays carried out in the presence of SAM and F^- (Fig. 2). A full kinetic characterization demonstrated that FIA-K237E had a k_{cat} of 0.20 ± 0.01 min^{-1}, very similar to the wild-type enzyme (Table 2). By contrast, the Michaelis constant (K_M) was higher (206.3 μM) than that of the wild-type FIA from *Streptomyces* sp. strain MA37 (3.7 μM). This experimental determination of kinetic parameters resulted in a catalytic efficiency (k_{cat}/K_M ratio) for the FIA-K237E fluorinase variant of 1 mM^{-1} min^{-1}. Together with the unaffected k_{cat} value and considering that the enzyme catalyses a single-step reaction, the observed increase in the Michaelis constant [defined as $K_M = (k_{-1} + k_{cat})/k_1$] could indicate increased dissociation of the substrate from the enzyme active site (represented by the k_{-1} component of K_M). The location of the residue at position 237 in the trimer:trimer interface, distal to the active site (Fig. 1B), suggests a long-range effect – plausibly resulting from increased flexibility of the trimeric form. Building on these experimental observations for the purified variant, we decided to explore if a trimer FIA mutant could be implemented for organofluorines biosynthesis as indicated in the next section.

Table 2. Kinetic constants of wild-type (WT) FIA and the engineered FIA-K237E variant.[a]

Fluorinase variant	K_M (μM)	k_{cat} (min^{-1})	k_{cat}/K_M (mM^{-1} min^{-1})
FIA (WT)	3.7 ± 0.7	0.22 ± 0.01	58
FIA-K237E	206.3 ± 34.1	0.20 ± 0.01	1

a. Kinetic constants were obtained from *in vitro* assays carried with purified enzymes. K_M and k_{cat} values are presented as averages ± standard deviation from at least triplicate determinations.

In vitro *synthesis of fluorometabolites using a trimeric fluorinase*

The successful engineering of a stable trimer (FIA-K237E) variant with a similar k_{cat} to the wild-type prompted us to explore this fluorinase for fluorometabolite synthesis in a biotransformation setup. To this end, cell-free extracts were prepared from cultures of *E. coli* BL21 transformed with plasmids encoding either FIA or FIA-K237E, where the expression of the cognate *flA* genes is driven by the T7 RNA polymerase (Fig. 5A). The resulting cell-free extracts were incubated in the presence of NaF and SAM for 20 h. After this incubation, the extracts were subjected to ^{19}F-NMR analysis and all fluorometabolites present in the samples were scanned. Figure 5B indicates that 5'-FDA was the main fluorometabolite in cell-free biotransformation experiments containing either FIA or FIA-K237E. As expected, no fluorinated species were detected in control conditions (i.e., cells transformed with an empty vector). Interestingly, we observed secondary peaks in the ^{19}F-NMR spectra (with a weak intensity), which likely correspond to ribose-based fluorometabolites (e.g., 5'-fluoro-5'-deoxy-D-ribose

© 2022 The Authors. *Microbial Biotechnology* published by Society for Applied Microbiology and John Wiley & Sons Ltd.,

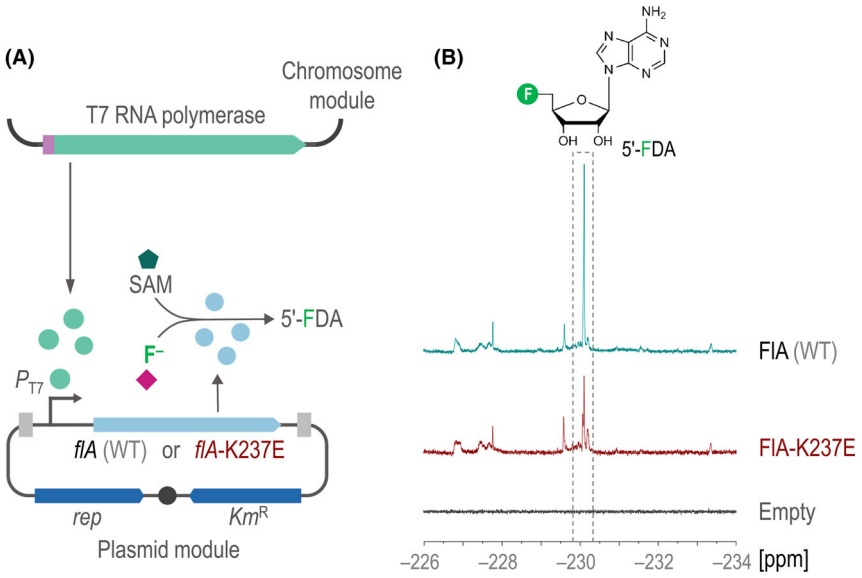

Fig. 5. *In vitro* synthesis of fluorometabolites by wild-type (WT) FIA and the rationally engineered FIA-K237E variant.
A. Scheme of the plasmid constructs used for cell-free biosynthesis of 5'-fluoro-5'-deoxyadenosine (5'-FDA), where the T7 RNA polymerase drives the expression of either *flA* (WT) or *flA*-K237E, placed under control of the P_{T7} promoter as a chromosomally integrated module. Abbreviations are *rep*, replication module; and Km^R, kanamycin-resistance determinant.
B. High-resolution ^{19}F-NMR profiles of the cell-free extracts upon incubation with NaF and *S*-adenosyl-L-methionine (SAM) as the substrate for FIA and FIA-K237E. *Empty* indicates a control experiment where the *E. coli* cells used to prepare the cell-free extract were transformed with the empty vector. Chemical shifts are expressed in parts per million, *ppm*.

1-phosphate). These fluorinated sugar derivatives could be potentially produced from 5'-FDA by endogenous *E. coli* enzymes, yet the most abundant organofluorine in these reactions was 5'-FDA. While further optimization would be needed to increase fluorometabolite titres using the trimeric FIA variant, these experiments indicate that the engineered FIA-K237E variant can be used for biotechnological purposes towards organofluorine production.

Discussion

Nature has widely adopted halogenation for tuning the physicochemical properties of secondary metabolites in a wide variety of microbial species – mostly through the introduction of chlorine and bromine atoms (Fejzagic *et al*., 2019; Neugebauer *et al*., 2019; Adak and Moore, 2021). This occurrence is reflected in the rich and diverse enzymology for such biohalogenations that continues to be revealed and harnessed for biotechnology (Latham *et al*., 2018; Cros *et al*., 2022). However, this state of affairs hardly extends to fluorination. Biosynthesis of organofluorines remains a significant challenge to biochemistry due to the particular properties of the F^- anion, which is a very poor nucleophile in water, and also because F has the highest oxidation potential of all of the halides (O'Hagan, 2008). These properties severely limit the potential for the creation of C–F bonds from F^- by either nucleophilic or electrophilic processes in an aqueous environment, and only the nucleophilic fluorinase enzyme is known so far in Nature to execute this chemistry. Rationally manipulating this enzyme thus emerges as the way forward to enrich the biosynthetic landscape of organofluorine production.

Here, we demonstrated rational manipulation of the oligomerization status of FIA through selecting and implementing mutations at the dimer interface of the native dimer of trimers. We further established that SAM binding is compromised to some extent in the obligate trimer, indicative of a relationship between quaternary structure and substrate channelling (Sweetlove and Fernie, 2018), although variants such as FIA-K237E still retained good capacity to synthesize fluorometabolites. From a broader perspective, engineering the oligomerization status of enzymes serves various purposes, both in fundamental and applied research (Liu *et al*., 2020). Forcing oligomerization is considered to be a viable strategy to improve enzyme function and stability under unfavourable environments (Yin *et al*., 2018; Jiang *et al*., 2019) – but this approach often complicates efforts in rationalizing functional enzyme characterization during fundamental research, which usually relies on assaying a mixture of oligomeric forms (Tong *et al*., 2005). A particularly relevant problem in biocatalysis using multimeric enzyme forms – in addition to the usually complex folding and assembling preparative processes involved – is the potential dissociation of enzyme subunits, which leads to deactivation and loss of activity, and even to

© 2022 The Authors. *Microbial Biotechnology* published by Society for Applied Microbiology and John Wiley & Sons Ltd.,

contamination of the final product(s) of interest (Katchalski-Katzir, 1993). In these cases, transforming homo-oligomeric enzymes into functional individual monomers facilitates protein engineering efforts to match the demands of both functional characterization and industrial applications. By the same token, working with individual monomers enable studies about oligomeric structure-activity relationships (Peverelli *et al*., 2016), and this general strategy has been applied in biomedicine for developing new drugs that target subunit interfaces of viral proteins (Sousa *et al*., 2011). Our present study not only provides evidence relevant for further functional studies of the fluorinase enzyme – an archetypal example of a homo-oligomeric enzyme for which the hexameric form was supposed to be an essential feature needed for catalysis – but it also leads to practical applications in fluorine chemistry.

Trimeric fluorinase variants may be implemented towards fluorometabolite biosynthesis in synthetic enzyme cascades, which are increasingly being used for producing complex molecules through pathways that would be difficult to implement in an *in vivo* system (Zhou *et al*., 2021). Additionally, it seems plausible that loosening interactions between the enzyme and its substrate(s), as we have done here by oligomerization engineering, may expand the substrate range. This potential broadening in substrate specificity could enable fluorination of substrates beyond SAM, thereby providing a direct route towards the biosynthesis of fluorinated drug synthons that contain aromatic moieties attached to sugars (Inoue *et al*., 2020). Such building blocks are usually prepared by indirect fluorination techniques based on diazotization of anilines or exchange fluorination of activated haloaromatics and, more recently, by developing new fluorinating agents incorporated in somewhat complex synthetic methods (Cheng and Ritter, 2019). In addition, the emerging catalytic features of novel FIA variants can be also exploited in combination with robust microbial hosts (Volke *et al*., 2020a; Nikel *et al*., 2021) that support the synthesis of fluorometabolites, compounds typically known to be toxic for the cells (Bitzenhofer *et al*., 2021). Taken these results together, our present study highlights that the construction of bacterial cell factories for fluorochemicals production involving FIA will benefit from manipulating a variety of parameters – including the enzyme oligomerization status *via* direct, rational protein engineering – for optimal catalytic performance.

Experimental procedures

Plasmid design and construction and general molecular biology procedures

Mutations were designed based on the structure of fluorinase from *Streptomyces* sp. strain MA37 (Deng *et al*., 2014) and sequence alignments to other fluorinases and the SAM-dependent SalL chlorinase (Eustáquio *et al*., 2008). Sequences were aligned and analysed using the Clustal Omega multiple sequence alignment tool (Larkin *et al*., 2007). The gene encoding FIA of *Streptomyces* sp. strain MA37 was obtained as a synthetic DNA fragment (Integrated DNA Technologies; Leuven, Belgium). The gene was cloned into a modified pET28(*a*)+ vector endowed with an *N*-terminal His-tag followed by a TEV (tobacco etch virus) cleavage site (GenScript; Piscataway, NJ, USA) with *USER* cloning. All primers were designed using the *AMUSER* tool (Genee *et al*., 2015). Phusion *U* DNA polymerase (Phusion *U* hot start master mix; ThermoFisher Scientific, Waltham, MA, USA) was used for PCR amplifications with the oligonucleotides listed in Table 3. PCR products were purified from a 1% (w/v) agarose gel and ligated with the *USER* enzyme to the receiving vectors using standard protocols (Sambrook and Russell, 2001; Ruiz *et al*., 2006; Volke *et al*., 2020b, 2021). Plasmids were transformed into chemically competent *E. coli* OneShot BL21(DE3) cells (ThermoFisher Scientific) for protein expression. Mutations were introduced in the *flA* sequence by PCR followed by *USER* cloning as described elsewhere (Volke *et al*., 2020c).

Protein production in E. coli *and protein purification protocols*

A single transformant *E. coli* colony carrying the construct of interest was used to inoculate 5 ml of lysogeny broth (LB) medium supplemented with kanamycin (50 mg l^{-1}) and grown overnight at 37°C. Next, 400 ml of LB medium supplemented with kanamycin (50 mg l^{-1}) was inoculated with the overnight culture at a 1% (v/v) ratio and cultures were incubated at 37°C until the optical density measured at 600 nm (OD_{600}) reached 0.5–0.8. At this point, protein production was induced by addition of 0.5 mM isopropyl-β-D-1-thiogalactopyranoside (IPTG; Sigma-Aldrich Co., St. Louis, MO, USA). Cultures were then allowed to grow overnight at 18°C, after which the cells were harvested by centrifugation (4000 *g*, 15 min, 4°C). Cell pellets were stored at −20°C prior to protein extraction and purification.

Cells and proteins were kept on ice or in the cold room throughout the purification process. Bacterial pellets were dissolved in washing buffer (50 mM HEPES, pH = 7.4, 300 mM NaCl and 20 mM imidazole) supplemented with protein inhibitor cocktail tablets (*cOmplete*™, EDTA-free protease inhibitor cocktail; Sigma-Aldrich Co.). Cells were lysed by three passes through an Emulsiflex C5 high-pressure homogenizer (Avestin Europe GmbH; Mannheim, Germany) and the lysate was cleared by centrifugation (12 000 *g*, 40 min, 4°C). The cleared

© 2022 The Authors. *Microbial Biotechnology* published by Society for Applied Microbiology and John Wiley & Sons Ltd.,

Table 3. Oligonucleotides used in this study.[a]

Name	Oligonucleotide sequence (5'→3')	Direction
flA	AGGGCCAUGCCGCCAACGGCAGCCAG	Forward
flA	AACGGGCCUCCACGCGCACCTTCAGGCC	Reverse
pET28	AGGCCCGTUGATCGAGCACCACCACCACC	Forward
pET28	ATGGCCCUGAAAATAAAGATTCTCGCCGC	Reverse
K237E	ATTAGGGUGATGGTTCACGTAGTGGGCC	Forward
K237E	ATCTCCAGGUGTTTGCCCTGGCCGATGC	Reverse
K237E	ACCTGGAGAUCATCCTGGACGACGTGCT	Forward
K237E	ACCCTAAUCAAGTTTTTTGGGGTCGAGGT	Reverse
D241A	ATTAGGGUGATGGTTCACGTAGTGGGCC	Forward
D241A	AGCACGUCGGCCAGGATGATCTTCAGGTGTT	Reverse
D241A	ACGTGCUGCCGTTCGAAGCCCCGCT	Forward
D241A	ACCCTAAUCAAGTTTTTTGGGGTCGAGGTGCC	Reverse
D241A+K237E	ATTAGGGUGATGGTTCACGTAGTGGGCC	Forward
D241A+K237E	AGGATGAUCTCCAGGTGTTTGCCCTGGCC	Reverse
D241A+K237E	ATCATCCUGGCCGACGTGCTGCCGTTCGAA	Forward
D241A+K237E	ACCCTAAUCAAGTTTTTTGGGGTCGAGGTG	Reverse
InsLS	ATTAGGGUGATGGTTCACGTAGTGGG	Forward
InsLS	ACTGACAGGUCGTCCAGGATGATCTTCA	Reverse
InsLS	ACCTGTCAGUGCTGCCGTTCGAAGCCCC	Forward
InsLS	ACCCTAAUCAAGTTTTTTGGGGTCGAGGTGCC	Reverse
K237E+N287P	ACCTGGAGAUCATCCTGGACGACGTGCT	Forward
K237E+N287P	AGTGGGUACGGATAGGCCAGGCTGG	Reverse
K237E+N287P	ACCCACUGAAAGCCGGCCTGAAGGT	Forward
K237E+N287P	ACCCTAAUCAAGTTTTTTGGGGTCGAGGT	Reverse
K237E+N287P	ATTAGGGUGATGGTTCACGTAGTGGGCC	Forward
K237E+N287P	ATCTCCAGGUGTTTGCCCTGGCCGATGC	Reverse

a. Oligonucleotides are named according to the intended mutation(s) introduced in FlA. Sequences containing *U* residues were used for *USER* cloning.

lysate was incubated with a Ni-NTA bead suspension (*HisPur*™ Ni-NTA resin, ThermoFisher Scientific; 1 ml per construct) during 1 h with gentle shaking. Beads were washed twice with wash buffer and the bound protein eluted with an elution buffer containing 50 mM HEPES (pH = 7.4), 300 mM NaCl and 300 mM imidazole. TEV-protease was added to the elution fractions (in a 1:20 fluorinase-to-TEV-protease ratio) and the resulting fractions were dialyzed against 20 mM HEPES (pH = 7.8), 50 mM NaCl, 1 mM DTT and 0.5 mM EDTA overnight. Samples were incubated again with 0.7 ml Ni-NTA beads (1 h) and the flow-through was collected. Beads were washed with wash buffer as indicated above, and the washed protein fractions were combined with the corresponding flow-through fractions. Protein purity was assessed using SDS-PAGE (*NuPAGE*™ 4–12% Bis-Tris protein gel; ThermoFisher Scientific). Finally, selected fractions were combined, and the buffer was exchanged to 20 mM HEPES (pH = 7.8), 150 mM NaCl and 3% (v/v) glycerol in centrifugal protein concentrators (10 000 Da cut-off; Amicon Ultra; Sigma-Aldrich Co.). Protein concentration was determined by assessing the absorbance at 280 nm in a NanoDrop™ 2000 spectrophotometer (ThermoFisher Scientific). Protein fractions were aliquoted, flash-frozen in liquid N_2 and stored at –20°C until further analysis.

Samples for SAXS measurement were further purified by size-exclusion chromatography using a Superdex™ 200 increase 10/300 GL column (30 cm×10 mm, 8.6 μm particle size; Sigma-Aldrich Co.) connected to an Äkta PURE™ system (Cytiva; Global Life Sciences Solutions, Marlborough, MA, USA) and eluted with a buffer containing 20 mM HEPES (pH = 7.4), 150 mM NaCl and 3% (v/v) glycerol. Fractions containing pure enzyme were pooled, concentrated and stored at 4°C until further use.

Size-exclusion chromatography

The oligomeric state of proteins was analysed using a Superdex™ 200 increase 10/300 GL column (30 cm×10 mm, 8.6 μm particle size; Sigma-Aldrich Co.) connected to an Äkta PURE™ system. Proteins were diluted in the running buffer (50 mM HEPES, pH = 7.8 and 150 mM NaCl) and centrifuged (17 000 *g*, 10 min, 4°C) before applying the sample to the column. The particle size was estimated by comparing the elution volumes to a commercial molecular weight maker (Gel filtration standard; BioRad Laboratories Inc., Hercules, CA, USA).

In vitro *enzyme activity assays*

Enzyme activity assays were carried out with 5 μM purified FlA or mutants thereof, mixed with 300 μM SAM (New England Biolabs, Ipswich, MA, USA) [or, in some cases, 300 μM of 5'-ClDA (Cayman Chemical Co., Ann

© 2022 The Authors. *Microbial Biotechnology* published by Society for Applied Microbiology and John Wiley & Sons Ltd.,

Arbor, MI, USA)] and 1 mM L-Met (Sigma-Aldrich Co.) in a buffer containing 30 mM HEPES (pH = 7.8), 150 mM NaCl and 75 mM KF. Reactions were incubated at 37°C for 4 h, with 80-μl samples taken at specific time points, incubated at 95°C for 5 min and centrifuged for 10 min at 17 000 *g*. The supernatants were analysed using an Eclipse Plus C18 column (100 × 4.6 mm, 3.5 μm particle size; Agilent Technologies, Santa Clara, CA, USA) connected to a HPLC system (Dionex™ *Ultimate* 3000; ThermoFisher Scientific) operated at a flow rate of 1 ml min^{-1}. A gradient of solvent A [0.05% (v/v) acetic acid in water] and B (acetonitrile) was implemented as follows: 5-12% (v/v) B in 1.5 min, 12% (v/v) B for 1 min, 12-30% (v/v) B in 2 min and 30-70% (v/v) B in 1.5 min. Enzyme kinetics were measured using 2 μM FlA or 1 μM mutants in a buffer containing 30 mM HEPES (pH = 7.8), 150 mM NaCl and 75 mM KF. The SAM concentration was varied between 0 and 800 μM, and samples were taken at specific time points. All samples were denatured by heating, and supernatants were analysed as explained above.

Data processing for (SEC)SAXS experiments

The ATSAS package was used for SAXS data processing and interpretation (Franke *et al*., 2017; Manalastas-Cantos *et al*., 2021). All raw data were radially averaged and buffer-subtracted automatically at the beamline. SEC-SAXS data were processed with CHROMIXS (Panjkovich and Svergun, 2018); concentration series were merged in Primus (Konarev *et al*., 2003). All data were quality checked with the AutoRg (Petoukhov *et al*., 2007) and GNOM (Svergun *et al*., 1988) software packages. Finally, theoretical scattering curves were generated and fitted to experimental data with the CRYSOL tool (Franke *et al*., 2017).

Biosynthesis of fluorometabolites in bacterial cell-free extracts

Cultures for production of wild-type FlA and its FlA-K237A derivative, as well as the corresponding cell-free extracts for fluorometabolite synthesis, were prepared as described above with the following minor modifications. Bacterial cell pellets were dissolved in wash buffer (50 mM HEPES, pH = 7.4 and 300 mM NaCl) and lysed by three passes through an Emulsiflex C5 homogenizer (Avestin Europe GmbH). Cell lysates were incubated with 2.5 U ml^{-1} of *Pierce*™ Universal Nuclease for cell lysis (ThermoFisher Scientific) for 30 min at room temperature under gentle shaking. The lysates were then centrifuged (10 000 *g*, 30 min, 4°C) and the corresponding supernatants were filtered (0.2 μm-pore size); the recovered cleared lysates were immediately used for *in vitro* synthesis of 5'-FDA. The *in vitro*, cell-free production of fluorometabolites was carried out in 20 ml-reactions containing 10 ml of cleared cell lysate, 5 mM NaF, 1 mM SAM and 50 mM potassium phosphate buffer (pH = 7.8) (Calero *et al*., 2020). Samples were statically incubated at 30°C for 20 h, and the reactions were stopped by heating at 95°C for 5 min, whereupon the resulting samples were stored at –20°C until further processing for fluorometabolite detection by NMR.

^{19}F-NMR analysis of fluorometabolites

Biological samples were lyophilized from a frozen solution in 50 mM potassium phosphate buffer using a Christ Alpha 1–2 LD Plus freeze dryer (Martin Christ Gefriertrocknungsanlagen GmbH, Osterode am Harz, Germany). To the freeze-dried sample was added a MeOD/D_2O solution (adjusted according to the sample size), and the resulting suspension was subjected to sonication to ensure dissolution of all fluorometabolites in the sample. After centrifugation (to remove any precipitate), ^{19}F-NMR experiments were recorded at 298 K on a Bruker AVANCE III HD instrument with either a SmartProbe BBFO$^+$ (for proton coupled experiments) or a TCI CryoProbe (for proton decoupled experiments), using $CFCl_3$ as an external reference (Calero *et al*., 2020; Wirth and Nikel, 2021).

Acknowledgements

The authors wish to thank Daniel C. Volke (DTU Biosustain, Denmark) and Isabel Pardo (CIB-CSIC, Spain) for helpful discussions. This work was funded by The Novo Nordisk Foundation grant to the Center for Biosustainability (NNF10CC1016517). P.I.N. was funded by grants from The Novo Nordisk Foundation (NNF20CC0035580, and *LiFe*, NNF18OC0034818), the European Union's Horizon 2020 Research and Innovation Programme under grant agreement No. 814418 (*SinFonia*) and the Danish Council for Independent Research (*SWEET*, DFF-Research Project 8021-00039B). T.K. and M.N.D. were funded by fellowships from the European Union's Horizon 2020 research and innovation program under the Marie Skłodowska Curie under grant agreement No. 713683 (*COFUNDfellowsDTU*).

Conflict of interest

None declared.

Author contributions

T.K., D.T., P.I.N., and D.H.W. were involved in conceptualization. T.K., P.T.L., P.C., and M.N.D. were involved in

© 2022 The Authors. *Microbial Biotechnology* published by Society for Applied Microbiology and John Wiley & Sons Ltd.,

data curation. T.K., F.F., D.H.W., M.N.D., P.T.L., and D.O. were involved in formal analysis. T.K., D.W., P.I.N., and D.O. acquired funding. T.K., F.F., D.H.W., P.T.L., P.C., and M.N.D. were involved in investigation. T.K., D.H.W., and P.I.N. developed methodologies. T.K., D.H.W., D.T., and P.I.N. were involved in project administration. D.H.W., P.I.N., D.T., and D.O. carried out supervision. T.K. and D.H.W. were involved in writing original draft, and P.I.N. was involved in writing. All authors were involved in writing and final editing.

References

Adak, S., and Moore, B.S. (2021) Cryptic halogenation reactions in natural product biosynthesis. *Nat Prod Rep* **38:** 1760–1774.

Bitzenhofer, N.L., Kruse, L., Thies, S., Wynands, B., Lechtenberg, T., Rönitz, J., *et al*. (2021) Towards robust *Pseudomonas* cell factories to harbour novel biosynthetic pathways. *Essays Biochem* **65:** 319–336.

Blanchet, C.E., and Svergun, D.I. (2013) Small-angle X-ray scattering on biological macromolecules and nanocomposites in solution. *Annu Rev Phys Chem* **64:** 37–54.

Calero, P., Volke, D.C., Lowe, P.T., Gotfredsen, C.H., O'Hagan, D., and Nikel, P.I. (2020) A fluoride-responsive genetic circuit enables *in vivo* biofluorination in engineered *Pseudomonas putida*. *Nat Commun* **11:** 5045.

Carvalho, M.F., and Oliveira, R.S. (2017) Natural production of fluorinated compounds and biotechnological prospects of the fluorinase enzyme. *Crit Rev Biotechnol* **37:** 880–897.

Cheng, Q., and Ritter, T. (2019) New directions in C-H fluorination. *Trends Chem* **1:** 461–470.

Cheng, X., and Ma, L. (2021) Enzymatic synthesis of fluorinated compounds. *Appl Microbiol Biotechnol* **105:** 8033–8058.

Cobb, S.L., Deng, H., McEwan, A.R., Naismith, J.H., O'Hagan, D., and Robinson, D.A. (2006) Substrate specificity in enzymatic fluorination. The fluorinase from *Streptomyces cattleya* accepts 2′-deoxyadenosine substrates. *Org Biomol Chem* **4:** 1458–1460.

Cros, A., Alfaro-Espinoza, G., de Maria, A., Wirth, N.T., and Nikel, P.I. (2022) Synthetic metabolism for biohalogenation. *Curr Opin Biotechnol* **74:** 180–193.

Deng, H., Cobb, S.L., McEwan, A.R., McGlinchey, R.P., Naismith, J.H., O'Hagan, D., *et al*. (2006) The fluorinase from *Streptomyces cattleya* is also a chlorinase. *Angew Chem Int Ed Engl* **45:** 759–762.

Deng, H., Ma, L., Bandaranayaka, N., Qin, Z., Mann, G., Kyeremeh, K., *et al*. (2014) Identification of fluorinases from *Streptomyces* sp. MA37, *Nocardia brasiliensis*, and *Actinoplanes* sp. N902–109 by genome mining. *ChemBioChem* **15:** 364–368.

Deng, H., O'Hagan, D., and Schaffrath, C. (2004) Fluorometabolite biosynthesis and the fluorinase from *Streptomyces cattleya*. *Nat Prod Rep* **21:** 773–784.

Dong, C., Huang, F., Deng, H., Schaffrath, C., Spencer, J.B., O'Hagan, D., and Naismith, J.H. (2004) Crystal structure and mechanism of a bacterial fluorinating enzyme. *Nature* **427:** 561–565.

Eustáquio, A.S., O'Hagan, D., and Moore, B.S. (2010) Engineering fluorometabolite production: fluorinase expression in *Salinispora tropica* yields fluorosalinosporamide. *J Nat Prod* **73:** 378–382.

Eustáquio, A.S., Pojer, F., Noel, J.P., and Moore, B.S. (2008) Discovery and characterization of a marine bacterial SAM-dependent chlorinase. *Nat Chem Biol* **4:** 69–74.

Fejzagic, A.V., Gebauer, J., Huwa, N., and Classen, T. (2019) Halogenating enzymes for active agent synthesis: first steps are done and many have to follow. *Molecules* **24:** e4008.

Franke, D., Petoukhov, M.V., Konarev, P.V., Panjkovich, A., Tuukkanen, A., Mertens, H.D.T., *et al*. (2017) *ATSAS 2.8*: a comprehensive data analysis suite for small-angle scattering from macromolecular solutions. *J Appl Crystallography* **50:** 1212–1225.

Gell, D.A., Grant, R.P., and Mackay, J.P. (2012) The detection and quantitation of protein oligomerization. *Adv Exp Med Biol* **747:** 19–41.

Genee, H.J., Bonde, M.T., Bagger, F.O., Jespersen, J.B., Sommer, M.O.A., Wernersson, R., and Olsen, L.R. (2015) Software-supported *USER* cloning strategies for site-directed mutagenesis and DNA assembly. *ACS Synth Biol* **4:** 342–349.

Goodsell, D.S., and Olson, A.J. (2000) Structural symmetry and protein function. *Annu Rev Biophys Biomol Struct* **29:** 105–153.

Inoue, M., Sumii, Y., and Shibata, N. (2020) Contribution of organofluorine compounds to pharmaceuticals. *ACS Omega* **5:** 10633–10640.

Jiang, W., Yang, R., Lin, P., Hong, W., and Fang, B. (2019) Bioinspired genetic engineering of supramolecular assembled formate dehydrogenase with enhanced biocatalysis activities. *J Biotechnol* **292:** 50–56.

Johnson, B.M., Shu, Y.Z., Zhuo, X., and Meanwell, N.A. (2020) Metabolic and pharmaceutical aspects of fluorinated compounds. *J Med Chem* **63:** 6315–6386.

Katchalski-Katzir, E. (1993) Immobilized enzymes—Learning from past successes and failures. *Trends Biotechnol* **11:** 471–478.

Konarev, P.V., Volkov, V.V., Sokolova, A.V., Koch, M.H.J., and Svergun, D.I. (2003) PRIMUS: a Windows PC-based system for small-angle scattering data analysis. *J Appl Crystallography* **36:** 1277–1282.

Larkin, M.A., Blackshields, G., Brown, N.P., Chenna, R., McGettigan, P.A., McWilliam, H., *et al*. (2007) Clustal W and Clustal X version 2.0. *Bioinformatics* **23:** 2947–2948.

Latham, J., Brandenburger, E., Shepherd, S.A., Menon, B.R.K., and Micklefield, J. (2018) Development of halogenase enzymes for use in synthesis. *Chem Rev* **118:** 232–269.

Liang, T., Neumann, C.N., and Ritter, T. (2013) Introduction of fluorine and fluorine-containing functional groups. *Angew Chem Int Ed Engl* **52:** 8214–8264.

Liu, H., Cao, M., Wang, Y., Lv, B., and Li, C. (2020) Bioengineering oligomerization and monomerization of enzymes: learning from natural evolution to matching the demands for industrial applications. *Crit Rev Biotechnol* **40:** 231–246.

Manalastas-Cantos, K., Konarev, P.V., Hajizadeh, N.R., Kikhney, A.G., Petoukhov, M.V., Molodenskiy, D.S., *et al*.

© 2022 The Authors. *Microbial Biotechnology* published by Society for Applied Microbiology and John Wiley & Sons Ltd.,

(2021) *ATSAS 3.0*: expanded functionality and new tools for small-angle scattering data analysis. *J Appl Crystallography* **54:** 343–355.

Markakis, K., Lowe, P.T., Davison-Gates, L., O'Hagan, D., Rosser, S.J., and Elfick, A. (2020) An engineered *E. coli* strain for direct *in vivo* fluorination. *ChemBioChem* **21:** 1856–1860.

Martinelli, L., and Nikel, P.I. (2019) Breaking the state-of-the-art in the chemical industry with new-to-Nature products *via* synthetic microbiology. *Microb Biotechnol* **12:** 187–190.

Meanwell, N.A. (2018) Fluorine and fluorinated motifs in the design and application of bioisosteres for drug design. *J Med Chem* **61:** 5822–5880.

Mei, H., Han, J., Fustero, S., Medio-Simon, M., Sedgwick, D.M., Santi, C., *et al*. (2019) Fluorine-containing drugs approved by the FDA in 2018. *Chemistry* **25:** 11797–11819.

Neugebauer, M.E., Sumida, K.H., Pelton, J.G., McMurry, J.L., Marchand, J.A., and Chang, M.C.Y. (2019) A family of radical halogenases for the engineering of amino-acid-based products. *Nat Chem Biol* **15:** 1009–1016.

Nieto-Domínguez, M., and Nikel, P.I. (2020) Intersecting xenobiology and *neo*-metabolism to bring novel chemistries to life. *ChemBioChem* **21:** 2551–2571.

Nikel, P.I., Fuhrer, T., Chavarría, M., Sánchez-Pascuala, A., Sauer, U., and de Lorenzo, V. (2021) Reconfiguration of metabolic fluxes in *Pseudomonas putida* as a response to sub-lethal oxidative stress. *ISME J* **15:** 1751–1766.

O'Hagan, D. (2008) Understanding organofluorine chemistry. An introduction to the C-F bond. *Chem Soc Rev* **37:** 308–319.

O'Hagan, D., and Deng, H. (2015) Enzymatic fluorination and biotechnological developments of the fluorinase. *Chem Rev* **115:** 634–649.

O'Hagan, D., Schaffrath, C., Cobb, S.L., Hamilton, J.T., and Murphy, C.D. (2002) Biochemistry: biosynthesis of an organofluorine molecule. *Nature* **416:** 279.

Panjkovich, A., and Svergun, D.I. (2018) CHROMIXS: automatic and interactive analysis of chromatography-coupled small-angle X-ray scattering data. *Bioinformatics* **34:** 1944–1946.

Petoukhov, M.V., Konarev, P.V., Kikhney, A.G., and Svergun, D.I. (2007) *ATSAS 2.1*–Towards automated and web-supported small-angle scattering data analysis. *J Appl Crystallography* **40:** s223–s228.

Peverelli, M.G., Soares da Costa, T.P., Kirby, N., and Perugini, M.A. (2016) Dimerization of bacterial diaminopimelate decarboxylase is essential for catalysis. *J Biol Chem* **291:** 9785–9795.

Pimviriyakul, P., Wongnate, T., Tinikul, R., and Chaiyen, P. (2020) Microbial degradation of halogenated aromatics: molecular mechanisms and enzymatic reactions. *Microb Biotechnol* **13:** 67–86.

Purser, S., Moore, P.R., Swallow, S., and Gouverneur, V. (2008) Fluorine in medicinal chemistry. *Chem Soc Rev* **37:** 320–330.

Ruiz, J.A., Fernández, R.O., Nikel, P.I., Méndez, B.S., and Pettinari, M.J. (2006) *dye* (*arc*) Mutants: insights into an unexplained phenotype and its suppression by the synthesis of poly(3-hydroxybutyrate) in *Escherichia coli* recombinants. *FEMS Microbiol Lett* **258:** 55–60.

Sambrook, J., and Russell, D.W. (2001) *Molecular Cloning: A Laboratory Manual*. Cold Spring Harbor: Cold Spring Harbor Laboratory.

Sousa, S.F., Tamames, B., Fernandes, P.A., and Ramos, M.J. (2011) Detailed atomistic analysis of the HIV-1 protease interface. *J Phys Chem* **115:** 7045–7057.

Sun, H., Yeo, W.L., Lim, Y.H., Chew, X., Smith, D.J., Xue, B., *et al*. (2016) Directed evolution of a fluorinase for improved fluorination efficiency with a non-native substrate. *Angew Chem Int Ed* **55:** 14277–14280.

Sun, H., Zhao, H., and Ang, E.L. (2018) A coupled chlorinase–fluorinase system with a high efficiency of trans-halogenation and a shared substrate tolerance. *Chem Commun* **54:** 9458–9461.

Svergun, D.I., Semenyuk, A.V., and Feigin, L.A. (1988) Small-angle-scattering-data treatment by the regularization method. *Acta Crystallogr A* **44:** 244–250.

Sweetlove, L.J., and Fernie, A.R. (2018) The role of dynamic enzyme assemblies and substrate channelling in metabolic regulation. *Nat Commun* **9:** 2136.

Tong, Y., Hughes, D., Placanica, L., and Buck, M. (2005) When monomers are preferred: a strategy for the identification and disruption of weakly oligomerized proteins. *Structure* **13:** 7–15.

Volke, D.C., Calero, P., and Nikel, P.I. (2020a) *Pseudomonas putida*. *Trends Microbiol* **28:** 512–513.

Volke, D.C., Friis, L., Wirth, N.T., Turlin, J., and Nikel, P.I. (2020b) Synthetic control of plasmid replication enables target- and self-curing of vectors and expedites genome engineering of *Pseudomonas putida*. *Metab. Eng. Commun* **10:** e00126.

Volke, D.C., Turlin, J., Mol, V., and Nikel, P.I. (2020c) Physical decoupling of XylS/*Pm* regulatory elements and conditional proteolysis enable precise control of gene expression in *Pseudomonas putida*. *Microb Biotechnol* **13:** 222–232.

Volke, D.C., Wirth, N.T., and Nikel, P.I. (2021) Rapid genome engineering of *Pseudomonas* assisted by fluorescent markers and tractable curing of plasmids. *Bio-protocol* **11:** e3917.

Wirth, N.T., and Nikel, P.I. (2021) Combinatorial pathway balancing provides biosynthetic access to 2-fluoro-*cis, cis*-muconate *in engineered Pseudomonas putida*. *Chem Catal* **1:** 1234–1259.

Wu, L., Maglangit, F., and Deng, H. (2020) Fluorine biocatalysis. *Curr Opin Chem Biol* **55:** 119–126.

Yin, L., Guo, X., Liu, L., Zhang, Y., and Feng, Y. (2018) Self-assembled multimeric-enzyme nanoreactor for robust and efficient biocatalysis. *ACS Biomater Sci Eng* **4:** 2095–2099.

Zheng, W., and Best, R.B. (2018) An extended Guinier analysis for intrinsically disordered proteins. *J Mol Biol* **430:** 2540–2553.

Zhou, Y., Wu, S., and Bornscheuer, U.T. (2021) Recent advances in (chemo)enzymatic cascades for upgrading bio-based resources. *Chem Commun* **57:** 10661–10674.

© 2022 The Authors. *Microbial Biotechnology* published by Society for Applied Microbiology and John Wiley & Sons Ltd.,